Study of impact of voltage gain of comparator on performance of newly designed functional generator

ŠOTNER, R.; JEŘÁBEK, J.; HERENCSÁR, N.

Optik
2018, vol. 172, November 2018, pp. 203-219

ISSN: 0030-4026

DOI: https://doi.org/10.1016/j.ijleo.2018.06.140

Accepted manuscript

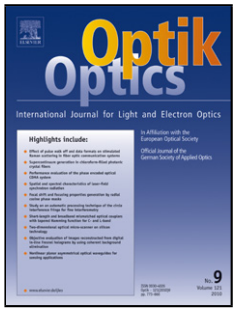

Title: Study of impact of voltage gain of comparator on performance of newly designed functional generator

Authors: Roman Sotner, Jan Jerabek, Norbert Herencsar

PII: S0030-4026(18)30950-1
DOI: https://doi.org/10.1016/j.ijleo.2018.06.140
Reference: IJLEO 61143

To appear in:

Received date: 4-5-2018
Accepted date: 28-6-2018

Please cite this article as: Sotner R, Jerabek J, Herencsar N, Study of impact of voltage gain of comparator on performance of newly designed functional generator, *Optik* (2018), https://doi.org/10.1016/j.ijleo.2018.06.140

Study of impact of voltage gain of comparator on performance of newly designed functional generator

Roman Sotner[1,2], Jan Jerabek[2], Norbert Herencsar[2]

[1]Dept. of Radio Electronics, Faculty of Electrical Engineering and Communication, Brno University of Technology, Technicka 3082/12, Brno, Czech Republic
[2]Dept. of Telecommunications, Faculty of Electrical Engineering and Communication, Brno University of Technology, Technicka 3082/12, Brno, Czech Republic

Abstract

This paper focuses on analysis of impact of voltage gain of comparator on features of designed triangular and sine wave generator. Newly designed generator employs minimal number of passive and active components based on simple voltage controllable amplifier and electronically controllable current conveyor or adjustable current amplifier. The generator has simple structure with easily available electronic control of repeating frequency and duty cycle. Detailed PSpice analyses of the modified generator are provided and relevant results of experimental measurements are shown. Discussion of non-ideal effects of voltage gain (*A*) of controllable amplifier used as comparator on generated amplitudes, on repeating frequency and on duty cycle as well as effects of statistical dispersion of important parameters are given. Observed behavior was analyzed not only by simulations but also by experimental measurements.

Keywords: Controllable current gain, electronic control, electronically controllable current conveyor, gain adjusting, voltage controllable amplifier, triangle and square wave generator.

1. Introduction

Electronic control of parameters in frame of active element [1] is very important for applications that require variable features. Applications that we discuss in this paper focus on triangle and square wave generators based on well-known solution [2] that is formed by loop connection of lossy integrator and comparator with two thresholds/hysteresis (so-called Schmitt trigger) [2]-[4]. Classical approaches employing operational amplifiers [2] are not very feasible because their controllable features are very restricted (only replacement of resistor in integrator by controllable equivalent) and complexity (number of passive elements - at least 3 resistor and floating capacitor) is higher in comparison to solutions utilizing other active devices as will be discussed in further text. Using of other active elements [1] allow us to obtain applications with simple control of their parameter(s).

Many solutions of generators in simple form based on modern active elements are available in recent literature [1]-[24]. The following text represents brief discussion of their complexity and building active elements used. Single current differencing transconductance amplifier (CDTA) and three resistors together with grounded capacitor create simple solution presented by Biolek et al. [5]. De Marcelis et al. [6] used two current conveyors of second generation (CCIIs) and six resistors together with floating capacitor in their topology. Two differential voltage current conveyors (DDCCs) complemented by three resistors and grounded capacitor are typical for solution introduced by Chien et al. [7]. Almashary et al. [8] contributed by simplified topology employing two CCIIs, three resistors and two grounded capacitors. Further simplification (also based on two CCIIs, three resistors and only one floating capacitor) was proposed by Pal et al. [9]. Circuit based on two current feedback operational amplifier (CFOAs) including four resistors and floating capacitor that was developed by Haque et al. [10] bring another benefit (low-impedance outputs). Two operational transresistance amplifiers (OTRAs) also offer features for design of generators as shown by Lo et al. [11] in topology utilizing three floating resistors and capacitor. Minaei et al. [12] tested combination of CFOAs and DVCCs in these constructions. All already discussed works

have limited availability of direct electronic tuning of repeating frequency (f_0). The adjusting of parameters of previously reported generators is not possible by control of internal parameters of active elements. The only way is intentional change of resistance value. Therefore, electronically adjustable solutions of generators were also introduced. Operational transconductance amplifiers (OTAs) offer simple direct electronic control of its internal parameter (transconductance) by DC bias current as shown for instance by Chung et al. [13] in topology implementing three OTAs, two grounded resistors and capacitor. Similar solution was presented by Siripruchyanun et al. [14]. Kumbun et al. [15] brought circuit based on two advanced active elements so-called multiple-output current through transconductance amplifiers (MO-CTTAs) where only one grounded capacitor is sufficient to create generator. Similarly, Silapan et al. [16] and Sristakul et al. [17] employ only two multiple-output current controlled current differencing amplifiers (MO-CCCDTAs) and grounded capacitor in their design. Universal current conveyor (UCC), CCII and eight passive (majority of them grounded) elements including four diodes were used by Janecek et al. [18]. Unfortunately, topologies introduced in [15]-[17] generate responses in form of current only and additional I→V transformation is necessary. The work [19] represents another approach into design of generators where differential output and fully balanced voltage differencing buffered amplifier (DO-VDBA, FB-VDBA) together with three grounded passive elements are used in order to obtain differential output waveforms. Solution presented in [20] focuses on application of so-called voltage differencing current conveyor (VDCC) with various methods of electronic controllability of parameters of generator. The topology may generate also differential-mode square-wave voltage but requires at least three passive elements incl. grounded capacitor. Generator introduced in [21] represents example of one of the simplest topologies (only single capacitor required as external subpart). However, active device used in [20], [21] itself is not commercially available and its emulation by accessible active subparts leads to very extensive circuitry [21]. Reference [22] deals with reconfigurability of the generator between exponential and linear charging/discharging. Special topology of electronically reconfigurable lossy/lossless integrator allows these features. Nevertheless, necessity of three active elements and four passive elements puts this circuit into the group of rather complex solutions. Detailed parameters of all discussed solutions are compared and summarized in **Table 1**.

Table 1. Comparison of discussed solutions.

Reference	No. of passive elements	No. of active elements	Grounded capacitor	Electronically tunable f_0	Trend of f_0 tuning (dep. of f_0 on driving force – resistance or active parameter)	Type of f_0 control (PE- passive elements; DC V - DC bias voltage; DC I - DC bias current)	f_0 tunable electronically without impact on duty cycle ≠ 50%	f_0 control without impact on duty cycle having no matching condition	Duty cycle control available (N/A – information not available)	Electronically controllable duty cycle	Duty cycle adjusted without additional circuitry (controlled DC current source)	Type of D control (PE- passive elements; DC V - DC bias voltage; DC I - DC bias current)	Type of output signals (current or voltage)
[5]	4	1	Yes	No	inversely proportional	PE	N/A	N/A	N/A	No	N/A	-	Voltages
[6]	7	2	No	No	inversely proportional	PE	N/A	N/A	N/A	No	N/A	-	Voltages
[7]	4	2	Yes	No	inversely proportional	PE	Yes	Yes	Yes	Yes	Yes	DC V	Voltages
[8]	5	2	Yes	No	inversely proportional	PE	N/A	N/A	N/A	No	N/A	-	Voltages
[9]	5(6)	2	No	No	inversely proportional	PE	N/A	N/A	N/A	No	N/A	-	Voltages
[10]	5	2	No	No	inversely proportional	PE	N/A	N/A	N/A	No	N/A	-	Voltages
[11]	4	2	No	No	inversely proportional	PE	N/A	N/A	N/A	No	N/A	-	Voltages
[12]	4	2	Yes	No	inversely proportional	PE	N/A	N/A	N/A	No	N/A	-	Voltages
[13]	3	3	Yes	Yes	linear	DC I	N/A	N/A	Yes	Yes	No	DC I	Voltages
[14]	3	3	Yes	Yes	linear	DC I	N/A	N/A	Yes	Yes	Yes	DC I	Voltages
[15]	1	2	Yes	Yes	linear	DC I	Yes	Yes	Yes	Yes	Yes	DC I	Currents
[16]	1	2	Yes	Yes	linear	DC I	N/A	N/A	N/A	No	N/A	-	Currents
[17]	1	2	Yes	Yes	linear	DC I	N/A	N/A	N/A	No	N/A	-	Currents
[18]	4	2	Yes	Yes	linear	DC V	N/A	N/A	N/A	No	N/A	-	Voltages
[19]	3	2	Yes	Yes	linear	DC I	Yes	No	Yes	Yes	No	DC I	Voltages
[20]	3	1	Yes	Yes	linear	DC I	Yes	No	Yes	Yes	No	DC I	Voltages
[21]	1	1	Yes	Yes	linear	DC I	Yes	No	Yes	Yes	No	DC I	Voltages
[22]	4	3	Yes	Yes	linear	DC V	N/A	N/A	No	No	N/A	-	Voltages
[23]	2	2	Yes	Yes	linear	DC V	Yes	Yes	Yes	Yes	No	DC I	Voltages
[24]	2	3	Yes	Yes	linear	DC V	Yes	No	Yes	Yes	Yes	DC V	Voltages
proposed	2	2	Yes	Yes	linear	DC V	Yes	Yes	Yes	Yes	Yes	DC V	Voltages

N/A – not available, not solved or not shown

As we can see from **Table 1**, circuit presented in this paper has really beneficial features because it provides all required features: a) low number of passive and active elements; b) electronic control of repeating frequency; c) electronic control of duty cycle (D); d) voltage signal at outputs. Both parameters (f_0, D) are controllably by DC voltage. **Table 1** indicates existence of even simpler solutions [15]-[17], [21] than those presented in this paper. However, duty cycle control is not allowed/studied in [16]-[17] and circuits provide output signals in form of current (additional conversion to voltage necessary). Simple topology utilizing single active device in [21] solves these drawbacks. Unfortunately, duty cycle control requires additional circuitry, i.e. additional specifically controlled DC current source (as in many cases included in **Tab. 1**) and proposed behavioral model of the active device is extremely complex. The most similar performance of the solution with low number of circuit components

has been achieved in [15]. Unfortunately, the circuit produces responses in form of currents. It requires additional conversion to voltage (by resistors) and buffering (low-impedance outputs) in comparison to our solution. Adjusting of parameters (repeating frequency, duty cycle) via DC driving voltage prepares solutions proposed in this paper for immediate implementation in analog/mixed systems without additional accessories or limitations. The solution presented in this paper is easily available by of-the-shelf active devices (no expensive IC fabrication of topology is required) and consist of acceptable amount of active and passive elements in comparison to other circuits listed in **Tab. 1**.

Goals of our design are to obtain very simple solutions with minimal number of external passive components. Experimental construction are based on commercially available devices. Research presented in this paper brings new beneficial structure including evaluation of practical impacts of real parameters of the generator. Presented circuit utilizes voltage controllable amplifier(s) for construction of Schmitt comparator [2]-[4] and electronically controllable current conveyor of second generation forming controllable loss-less integrators. Some practical/real properties are quite hidden if only brief and superficial study is done, but these features are important for estimation of expected behavior of application. Simulations and real experiments confirm operability that highly depends on real features of active elements, especially in case of very simple circuits. This was found as the most important disadvantage and was deeply investigated in this paper.

Paper is organized as follows: Section 1 briefly summarizes recent progress in the field of adjustable generators. Section 2 explains theoretical behavior of generator based on well-known structure (comparator-integrator) and modern electronically adjustable active elements. In this paper, we present interesting solution of simple triangular and square wave generator overcoming features of the most similar previously reported solutions [23]-[24] with useful controllable parameters that are analyzed in section 3. Section 4 investigates features by PSpice simulations and studies practical impacts of most influencing features of active elements (comparator especially) on generator performance. Section 5 deals with experimental results of laboratory tests in order to confirm behavior expected from simulations. Conclusion and summarization is given in section 6.

2. Construction details of the generator

Block diagram of the generator is shown in **Fig. 1**. Unfortunately, classical structure employing loss-less integrator and Schmitt trigger (comparator) [2]-[4] based on operational amplifiers does not allow direct electronic control of parameters of generated signal and it is therefore outdated by modern solutions.

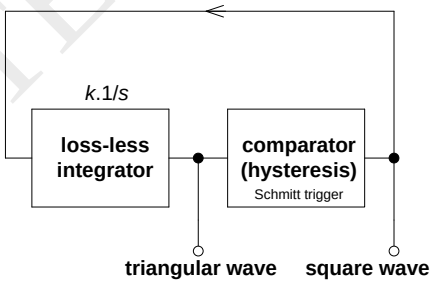

Figure 1. Basic block diagram of the triangular and square wave generator.

Our effort focuses on electronic control of parameters of application. Therefore, we prefer active elements that allow adjusting of their important parameters electronically (by external control force, in our case DC voltage). Voltage controllable (variable gain) amplifiers (VCAs) are very important for design of modern analog systems. They offer wide range of gain control (-40 dB to 40 dB for example [25]), high slew rate and bandwidth and they are available commercially (many types are digitally controllable – it gives direct control of application from microcontroller for example). There are also some types of current amplifiers (CA) [26], [27] and simple controllable current conveyors [28], [29] available and they allow synthesis and design of interesting and simple integrator circuits. We selected useful examples of discussed active elements for further design of generator, namely: voltage controllable amplifier VCA810 [25], and current-mode multiplier EL2082 [30] as electronically

controllable current conveyor (ECCII) [31]-[33]. Gains of voltage controllable amplifier (A) and electronically controllable current conveyor (B) are controlled by DC voltage.

The loss-less inverting integrators are the key parts of generators. Loss-less inverting integrator based on discussed adjustable-gain devices is shown in **Fig. 2**.

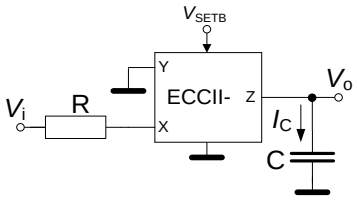

Figure 2. Controllable loss-less inverting integrators used in proposed generator using ECCII.

Ideal voltage transfer of the integrator shown in **Fig. 2** has very simple form:

$$K_{\text{int}}(s) = -\frac{B}{sRC} \cong -\frac{V_{SETB}}{sRC}. \tag{1}$$

The DC control voltage V_{SETB} shown in (1) is set in accordance to [30] (approximately valid $B \cong V_{SETB}$ for $V_{SETB} \leq 2$ V).

Construction of the simplest solution of comparator (Schmitt trigger) [2]-[4], which is required for these types of generators, is shown in **Fig. 3**, where VCA element is utilized with full positive feedback without any additional resistors. The output voltage (V_o) reaches two saturation levels ($\pm V_{sat\_VCA}$) as clear from **Fig. 4**. These levels can by defined by catalogue parameters [25] or also experimentally [23], [24].

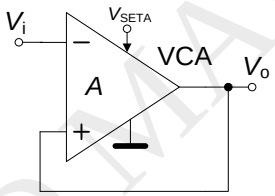

Figure 3. The simplest solution of comparator employing VCA with positive feedback.

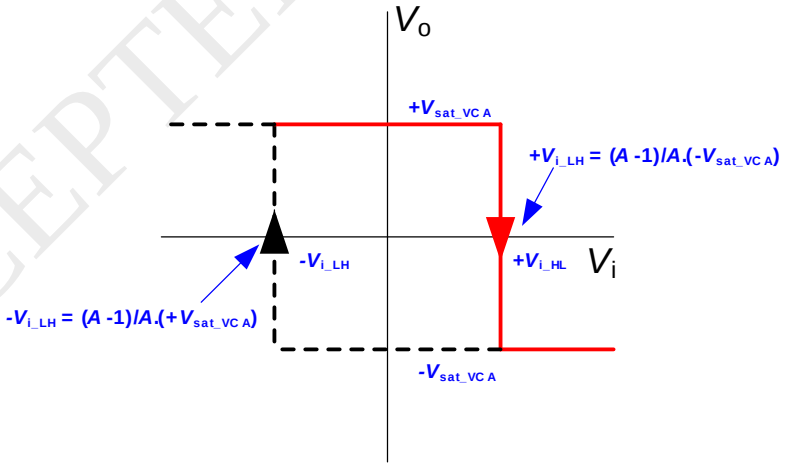

Figure 4. DC transfer characteristics of the Schmitt comparator with hysteresis based on VCA.

Output voltages $\pm V_{sat\_VCA}$ of the comparator are determined by both input threshold voltages ($\pm V_i = +V_{i\_HL} = -V_{i\_LH}$) as:

$$\pm V_{sat\_VCA} = \frac{A}{A-1}(\mp V_i) \cong \frac{10^{-2(V_{SETA}+1)}}{10^{-2(V_{SETA}+1)}-1}(\mp V_i). \tag{2}$$

The reference voltages (input thresholds – crossing of these values causes turnover of output voltage from positive to negative saturation respectively) increase for higher value of gain A and are equal to V_{sat_VCA} for $A \rightarrow -\infty$.

3. The generator analysis

In accordance to general topology presented in **Fig. 1**, we proposed and tested three suitable solutions based on components described above that offer electronic control of repeating frequency (f_0) and possibility of duty cycle (D) adjusting. The circuit shown in **Fig. 5** uses inverting integrator from **Fig. 3**, comparator from **Fig. 4** and requires only two passive elements. The duty cycle is now controlled by DC voltage at Y terminal of ECCII, which decreases the complexity in comparison to the similar solutions [23], [24]. The diagram of parameters of output waveforms and time sections for following analysis and derivation is given in **Fig. 6**.

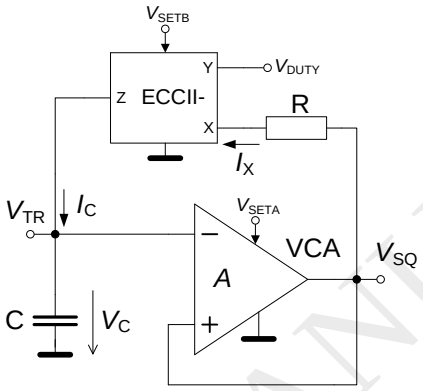

Figure 5. The second solution of the generator employing also ECCII and VCA active elements.

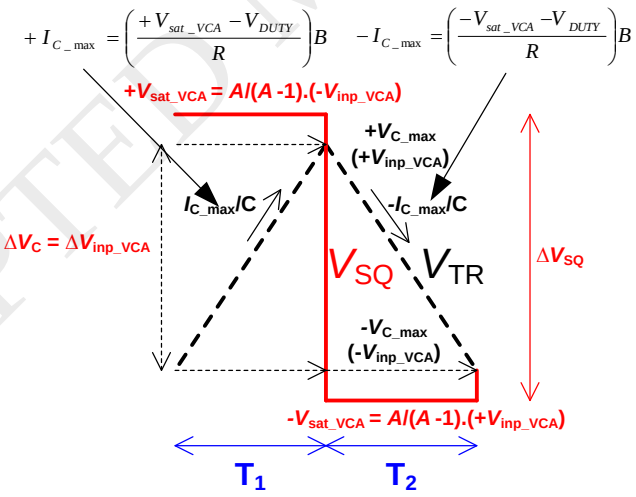

Figure 6. Diagram of parameters of output waveforms, time sections and thresholds.

The maximum of current flowing through capacitor is limited by $1/R$ to value derived from V_{SQ} and current gain B of current amplifier section. The linear dynamic range of current amplifier is supposed as sufficient for this operation. The current limitation occurs for higher input level than saturation limit represented by V_o (VCA in **Fig. 3**). Current gain is low and dynamics/linearity of current amplifier is favorable. Therefore, saturation of the ECCII (current amplifier part) influences charging of capacitor C minimally. Based on principle of current/voltage transformation between Y and X terminals of ECCII- in **Fig. 5**, the following relation:

$$RI_X + V_{DUTY} = V_{SQ}, \tag{3}$$

results into:

$$V_{SQ} - V_{DUTY} = \frac{R}{B} I_Z = \frac{R}{B} I_C , \tag{4}$$

when definition of current transfer between X and Z terminal of ECCII- is considered. Then, the maximal current levels through C can be expressed as:

$$+ I_{C\_\max} = \left(\frac{+V_{sat\_VCA} - V_{DUTY}}{R} \right) B , \tag{5}$$

$$- I_{C\_\max} = \left(\frac{-V_{sat\_VCA} - V_{DUTY}}{R} \right) B , \tag{6}$$

where limitation of V_{SQ} (V_{sat_VCA}) is given by saturation level of VCA [25] and, therefore, also threshold voltages highly depend on gain A (2). The linear change of voltage across the capacitor from $-V_{C\_max}$ to $+V_{C\_max}$ (thresholds of the comparator) can be expressed as:

$$\Delta V_{TR} = \Delta V_C = +V_{C\_\max} - (-V_{C\_\max}) = 2V_{C\_\max} . \tag{7}$$

Voltage change of V_{SQ} (V_{sat_VCA}) can be achieved analogously as:

$$\Delta V_{SQ} = +V_{sat\_VCA} - (-V_{sat\_VCA}) = 2V_{sat\_VCA} . \tag{8}$$

We can use equation (2) to obtain the following form for relation between ΔV_{TR} and ΔV_{SQ} as:

$$\Delta V_{TR} = \left(\frac{A-1}{A} \right) \Delta V_{SQ} . \tag{9}$$

Because $\Delta V_{TR} = 2V_{C\_max}$, $\Delta V_{SQ} = 2V_{sat\_VCA}$, it can be rewritten also as:

$$+V_{C\_\max} = \left(\frac{A-1}{A} \right) \left(-V_{sat\_VCA} \right) , \tag{10}$$

$$-V_{C\_\max} = \left(\frac{A-1}{A} \right) \left(+V_{sat\_VCA} \right) , \tag{11}$$

$$2V_{C\_\max} = \left(\frac{A-1}{A} \right) 2V_{sat\_VCA} . \tag{12}$$

The equation for repeating frequency can be easily derived from linear voltage increase or decrease across capacitor (between $\pm V_{C\_max}$) by help of (5), (6), (12) as:

$$2V_{sat\_VCA} \left(\frac{A-1}{A} \right) = \frac{I_{C\_\max}}{C} T_1 , \tag{13}$$

$$2V_{sat\_VCA} \left(\frac{A-1}{A} \right) = -\frac{I_{C\_\max}}{C} T_2 , \tag{14}$$

resulting into:

$$2V_{sat\_VCA} \left(\frac{A-1}{A} \right) = \frac{(V_{sat\_VCA} - V_{DUTY})B}{RC} T_1 , \tag{15}$$

$$2V_{sat\_VCA} \left(\frac{A-1}{A} \right) = \frac{(V_{sat\_VCA} + V_{DUTY})B}{RC} T_2 , \tag{16}$$

Then both intervals are given by:

$$T_1 = \frac{2V_{sat\_VCA}\left(\frac{A-1}{A}\right)RC}{\left(V_{sat\_VCA} - V_{DUTY}\right)B}, \tag{17}$$

$$T_2 = \frac{2V_{sat\_VCA}\left(\frac{A-1}{A}\right)RC}{\left(V_{sat\_VCA} + V_{DUTY}\right)B}. \tag{18}$$

The repeating frequency ($f_0 = 1/(T_1+T_2)$) and duty cycle ($D = T_1/T$, period $T = T_1 + T_2$) can be expressed as:

$$f_0 = \frac{B\left(V_{sat\_VCA} + V_{DUTY}\right)\left(V_{sat\_VCA} - V_{DUTY}\right)}{4RC\left(V_{sat\_VCA}\right)^2\left(\frac{A-1}{A}\right)} \cong \frac{V_{SETB}\left(V_{sat\_VCA} + V_{DUTY}\right)\left(V_{sat\_VCA} - V_{DUTY}\right)}{4RC\left(V_{sat\_VCA}\right)^2\left(\frac{A-1}{A}\right)}, \tag{19}$$

$$D = \frac{T_1}{T} = \frac{1}{2}\left(1 + \frac{V_{DUTY}}{V_{sat\_VCA}}\right). \tag{20}$$

The V_{DUTY} voltage may influence repeating frequency. However, when D is set to specific value the parameter suitable for f_0 control (B, V_{SETB} respectively) cannot have impact on D that is significant advantage.

4. Detailed PSpice analysis of the solution

Macromodels of EL2082 [30] and VCA810 [25] devices are used in the following analyses. Selected parameters (expected as design constants) are as follows: R = 390 + 95 Ω (intrinsic resistance of current input of EL2082 is 95 Ω [34]), C = 100 pF + 6 pF (parallel combination of parasitic capacitance of EL2082 output and parasitic capacitance of input of VCA610 is 6 pF [34], [28]). Adjustable parameters were initially set to: B = 0.2 (V_{SETB} = 0.2 V), A = 5 (V_{SETA} = -1.35 V), term $A/(A\text{-}1)$ = 1.25, D = 50% (V_{DUTY} = 0 V). Expected f_0 (including 6 pF parasitic capacitance) has value 1.216 MHz.

We have tested features of the comparator (VCA) in detail. Simulated DC characteristic of the VCA-based comparator for our initial values (A = 5) is presented in **Fig. 7**. Gain A has direct impact on threshold voltages and saturation corners as we have already discussed in previous text. Stepping of A (V_{SETA}) and its influence on threshold and saturation levels is documented in **Fig. 8**. This behavior affects accuracy of f_0 as well as D because both parameters depend on V_{sat_VCA}, see (19) and (20).

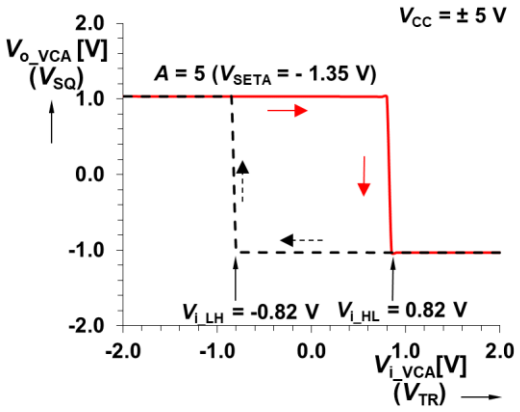

Figure 7. Simulated DC transfer characteristic of Schmitt comparator based on single VCA.

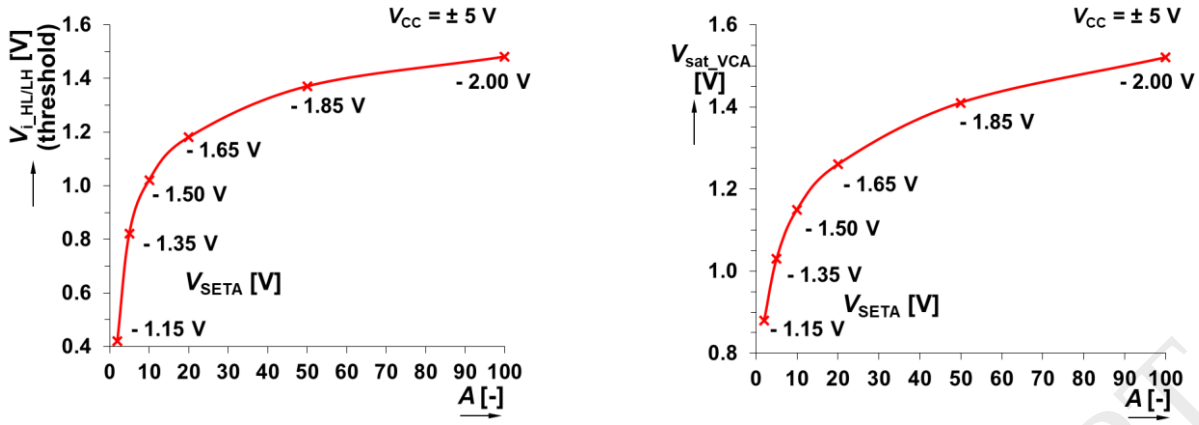

a) b)

Figure 8. Simulated influence of gain *A* on: a) threshold voltages, b) output saturation levels.

Simulated transient responses of the generator is shown in **Fig. 9**. Tuning of f_0 of the generator by *B* (V_{SETB}) for two discrete frequencies 1.217 MHz (V_{SETB} = 0.2 V) and 5.121 MHz (V_{SETB} = 1 V) is demonstrated in **Fig. 10**. Dependence of f_0 on *B* (V_{SETB}) is shown in **Fig. 11**. Tuning of f_0 was tested from 0.63 to 7.05 MHz by *B* changed from 0.1 to 1.5 (V_{SETB} equal to 0.1 - 1.5 V [30]). Estimated trace in **Fig. 12** takes *C* = 106 pF (6 pF parasitic) into calculation. Output amplitudes and their variation during the tuning process are given in Fig. 18, all for initial setting of comparator (*A* = 5).

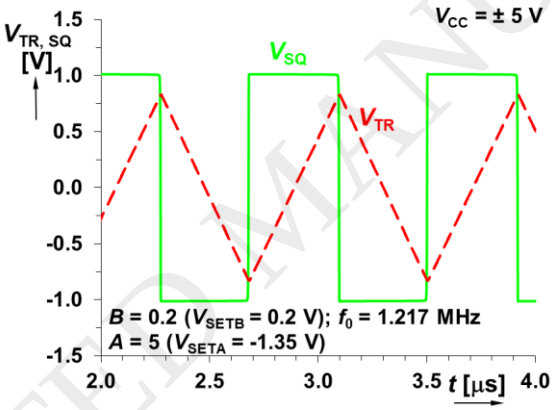

Figure 9. Transient responses of both generated signals.

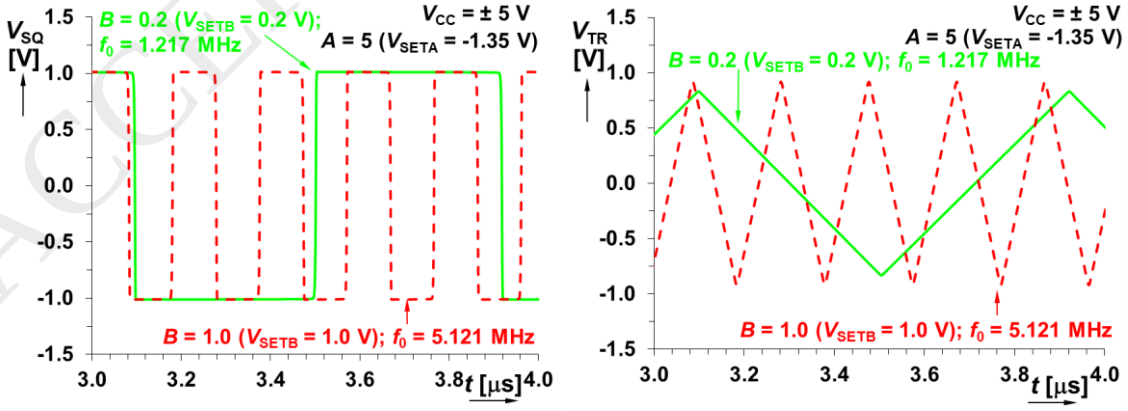

a) b)

Figure 10. Square wave transient responses for two discrete frequencies: a) triangular wave, b) square wave.

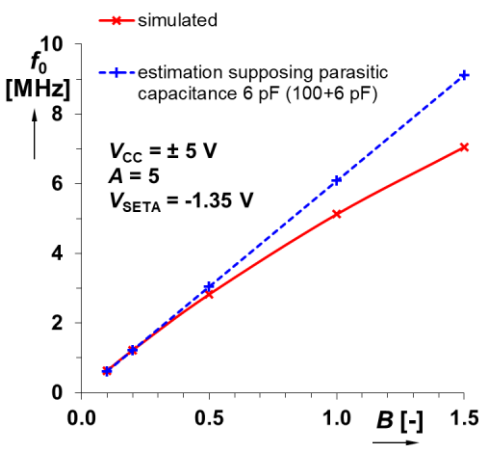

Figure 11. Dependence of repeating frequency on current gain B (estimation supposes only additional 6 pF parasitic capacitance in calculation – 100 + 6 pF).

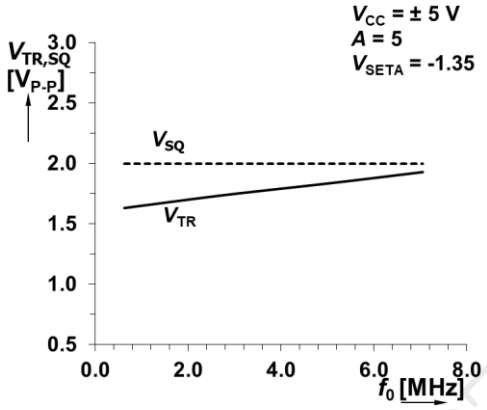

Figure 12. Dependence of output levels on repeating frequency.

Duty cycle can be easily controlled by V_{DUTY} as is shown in **Fig. 13**, where two discrete values of D = 27% and 93% (V_{DUTY} = -0.5 and 0.9 V) are shown on square wave response. Repeating frequency of generated waveform with specific D can be tuned independently on D as shows Fig. 20. Duty cycle was set to 93% (V_{DUTY} = 0.9 V) and f_0 achieved values 0.292 MHz (V_{SETB} = 0.2 V) and 1.253 MHz (V_{SETB} = 1.0 V). **Figure 14** illustrates dependence of D on V_{DUTY}, which was verified from 8% to 93% by V_{DUTY} driven from -0.9 to +0.9 V.

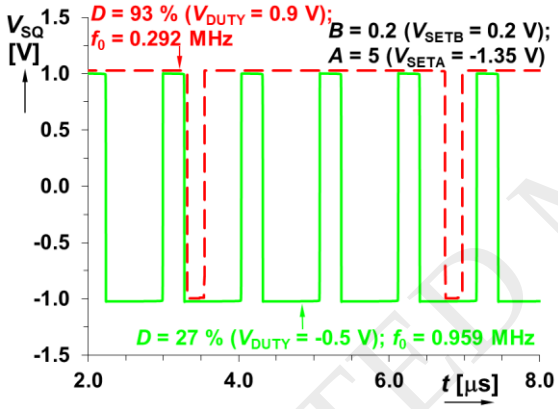

Figure 13. Examples of the control of the duty cycle for two discrete values of V_{DUTY}.

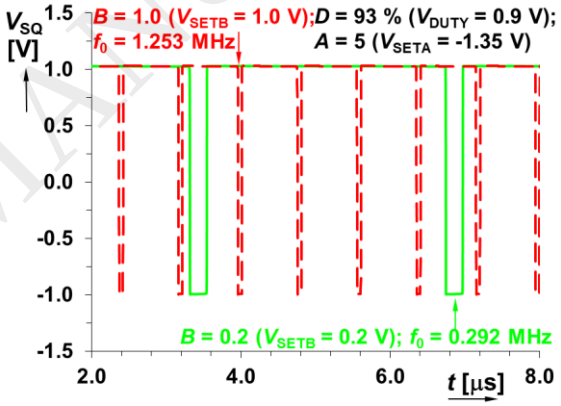

Figure 14. Example of f_0 control independently on set value of D by V_{DUTY}.

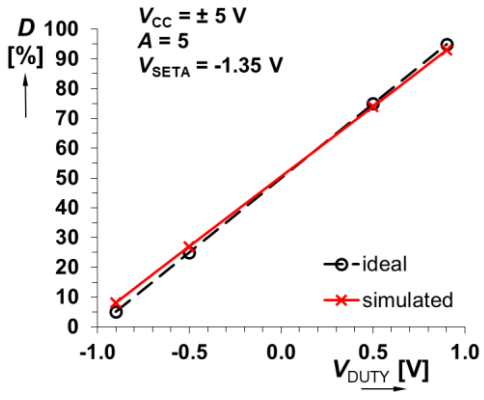

Figure 15. Dependence of D on V_{DUTY}.

Behavior and accuracy of the comparator (V_{sat_VCA} and threshold dependence on the gain A as we have shown in **Fig. 8**) has direct impact on obtained f_0 and generated amplitudes as expected from theory. Impact of A (V_{SETA}) on f_0 can be observed in **Fig. 16**. It is obvious that when gain A overcomes certain limit, it leads to minimal impact on f_0. However, lower A allows to obtain quite high value of f_0 for relatively very low gain B (V_{SETB}) in ranges below 1. It is the reason why we designed generator with gain A = 5. Similarly, impact of A on levels of generated signals is shown in **Fig. 17**. Impact of A changes on D is typical for different D than 50%, see example in **Fig. 18**. Despite discussed behavior, the low value of A helps to obtain the highest possible operational repeating frequency (see **Fig. 16**, it will be proven also in experiments, section 5) that can be useful in some cases (variation of the amplitude can be removed by passive diode limiter connected at the comparator output).

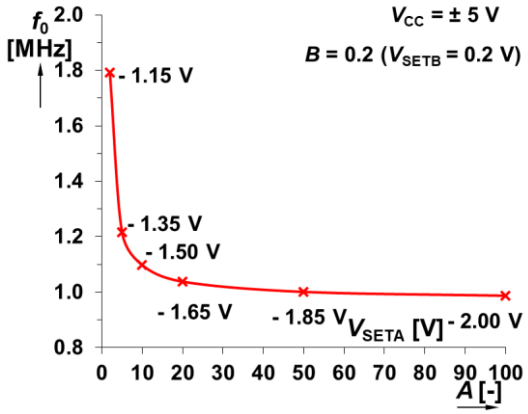

Figure 16. Influence of A (VCA) on f_0.

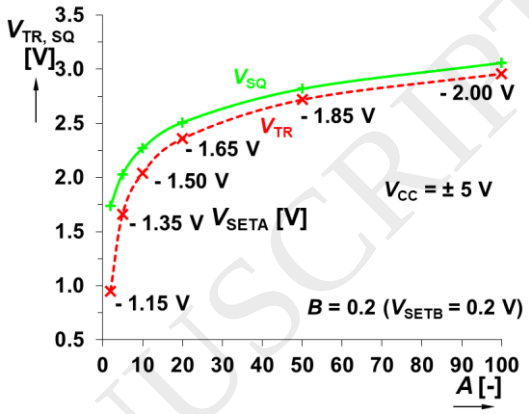

Figure 17. Influence of A (VCA) on generated levels.

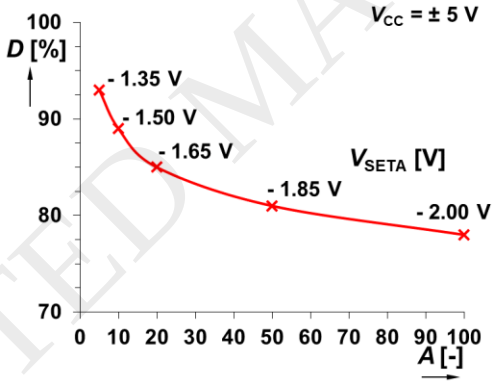

Figure 18. Influence of A (VCA) on D (initial/nominal D = 93%).

Statistical results of Monte Carlo analysis in order to observe dispersion of f_0 are given in **Fig. 19**. Tolerances of important circuit parameters were selected as follows: 1% R, 5% C, and 10% of V_{SETB}, V_{SETA} at f_0 = 1.217 MHz (V_{SETB} = 0.2 V, V_{SETA} = -1.35 V), value of duty cycle was expected as D = 50% (V_{DUTY} = 0 V). Dispersion (sigma) was found as Δf_0 = 137 kHz, see details in **Fig. 19**. First of all, accuracy of f_0 is strongly dependent on A (V_{SETA}) as we have already shown several times. The same analyses were provided for D = 93% (V_{DUTY} = 0.9 V), f_0 = 0.292 MHz and 20% tolerance of V_{DUTY}. Results are shown in **Fig. 20** and **Fig. 21** where dispersion Δf_0 = 126 kHz and ΔD = 3% is observed.

Behavior of the generator was also tested under condition of A = 50 (V_{SETA} = -1.85 V). Results of Monte Carlo analysis confirm presumption and f_0 dispersion is substantially lower Δf_0 = 39 kHz (but f_0 has slightly different value 1 MHz) than in previous case (A = 5), see **Fig. 22**.

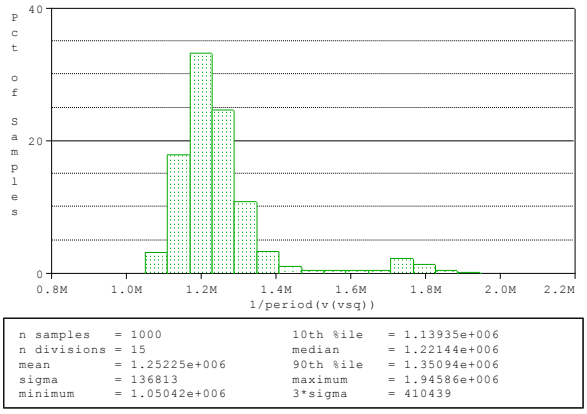

Figure 19. Monte Carlo analysis of f_0 dispersion (D = 50%).

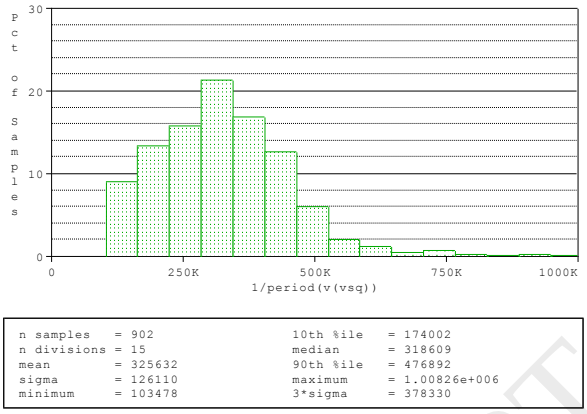

Figure 20. Monte Carlo analysis of f_0 dispersion (D = 93%, V_{DUTY} = 0.9 V).

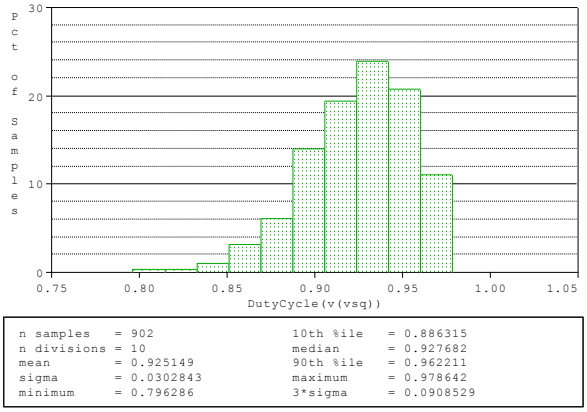

Figure 21. Monte Carlo analysis of D dispersion (initial D = 93%, V_{DUTY} = 0.9 V).

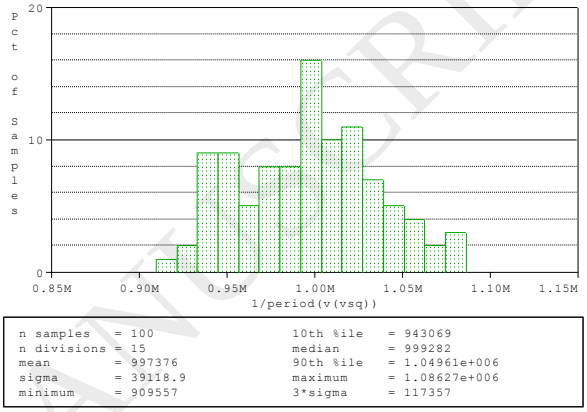

Figure 22. Monte Carlo analysis of f_0 dispersion for A = 50 (D = 50%).

5. Experimental results

Features of simulated solution of the waveform generator were verified also by laboratory experiments. These tests verified functionality of the concept deeply. Experiments reveal significant inaccuracy of the PSpice model of VCA810 from real device, especially in case of transfer performances and saturation limits (compare **Fig. 17** and traces in **Fig. 27**) in case of large signals at high frequencies especially (incl. slew-rate). These inaccuracies are really important for prediction of threshold voltages and output saturation levels of the comparator based on VCA in surveyed operational frequency band. Dependencies of repeating frequency f_0 on current gain in measured cases valid for several values of V_{SET_A} (influencing comparator) are given in **Fig. 23**. Comparing ideal, simulated and measured traces, the best fitting curve was obtained for V_{SETA} = -1.2 V (supposed small-signal A = 2.5), see **Fig. 24**.

In order to demonstrate differences between characteristics of generated signals, **Fig. 25** covering four settings of V_{SETA} was prepared. Transient responses for four values of V_{SETA} (-1.35 V, -1.25 V, -1.20 V, -1.15 V) are compared in **Fig. 25**. The best shape of the square wave output signal is obtained for V_{SETA} = -1.35 V. However, the repeating frequency has the lowest value. The highest f_0 is available for V_{SETA} = -1.15 V but output level is the lowest from all tested values of V_{SETA} and shape of square wave is not satisfactory. **Figure 25** shows these results. Change of frequency f_0 was expected from **Fig. 16**, change of output level from **Fig. 8**.

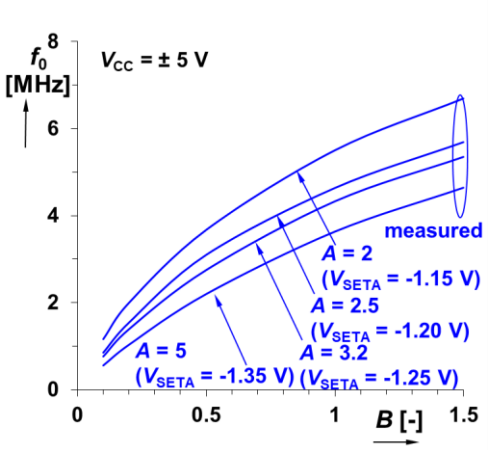

Figure 23. Selected measured dependencies of f_0 on current gain B for different V_{SETA} in comparison with simulation results.

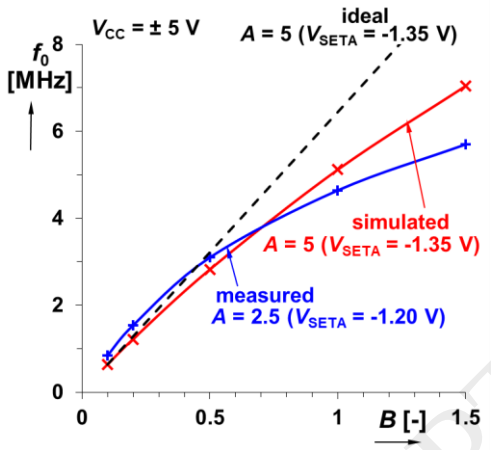

Figure 24. Illustration of ideal, simulated and the best fitting measured dependence of f_0 on B.

Impact of voltage gain A value of the comparator on f_0 was studied and results are shown in **Fig. 26** where detail of dependency of f_0 on supposed A for above noted range of V_{SETA} (all for $B = 0.2$) can be seen as well as dependence of the output levels on A (V_{SETA}) in **Fig. 27**.

As already described, duty cycle of generated signal can be easily controlled by DC voltage applied to Y terminal of ECCII in the generator structure. However, previously discussed features influence also this parameter. **Figure 28** presents comparison of ideal, simulated and measured dependence of duty cycle on V_{DUTY}. The examples of transient responses for different D than 50 % are given in **Fig. 29** and **Fig. 30**. The minimal and maximal available D (almost 5 and 95 %) can be reached for $V_{DUTY} \cong \pm 1.5$ V (see **Fig. 32**, where screens for $D = 5.1\%$ are shown). Uncertainty of gain A setting by V_{SETA} for higher frequencies and the same reasons as discussed above (uncertainty of thresholds and V_{sat_VCA}) causes mismatch between simulation and real experiments (see **Fig. 28**). **Figure 31** evaluates dependencies of output levels (peak-to-peak) on f_0, V_{SETA} is parameter of each trace.

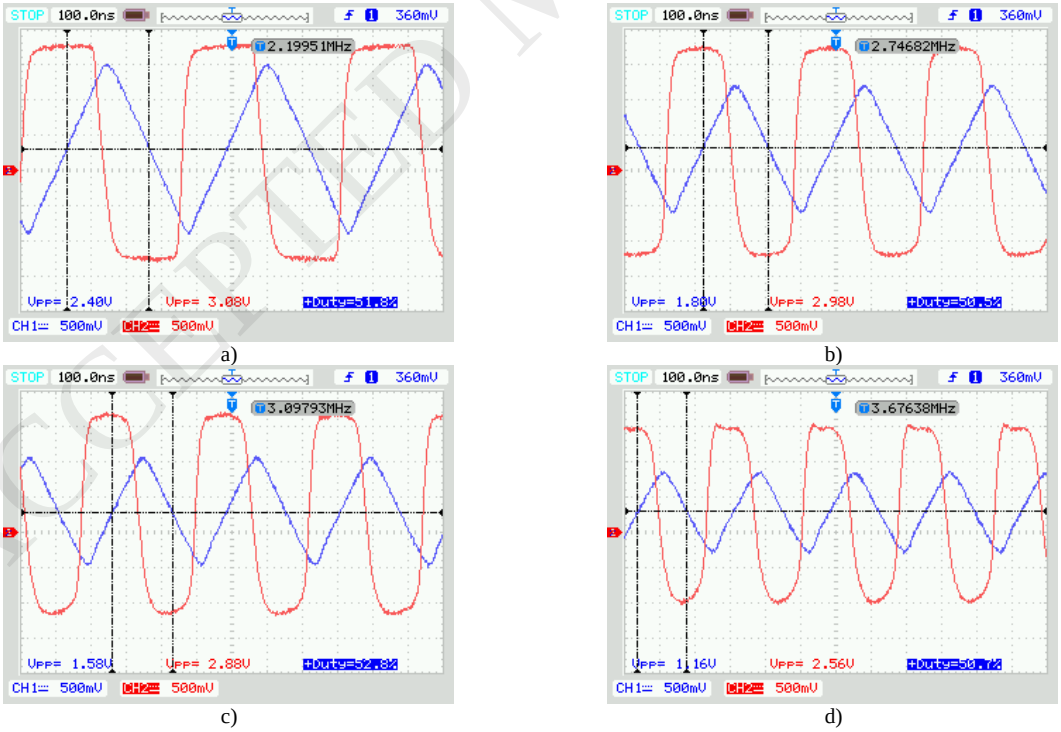

Figure 25. Measured output transient responses: a) V_{SETA} = -1.35 V, b) V_{SETA} = -1.25 V, c) V_{SETA} = -1.20 V, d) V_{SETA} = -1.15 V.

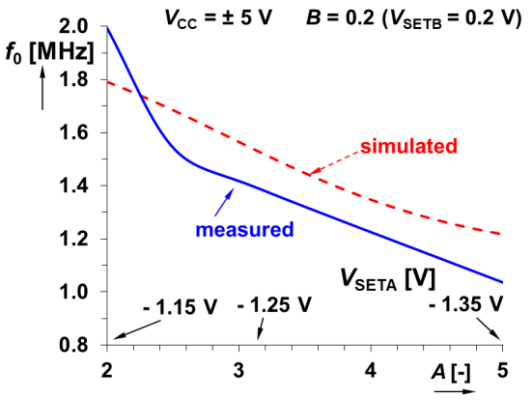

Figure 26. Detailed comparison of simulated and measured dependence of f_0 on A.

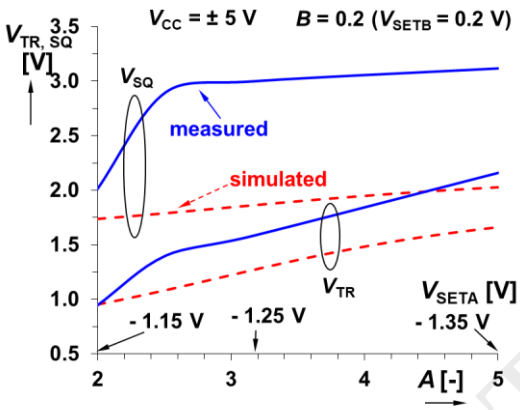

Figure 27. Detailed comparison of simulated and measured dependence of output levels on A.

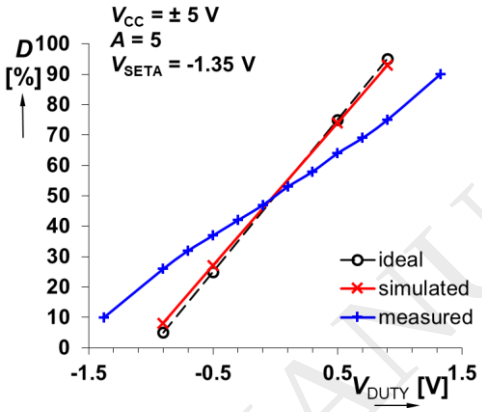

Figure 28. Comparison of ideal, simulated and measured dependence of duty cycle on V_{DUTY}.

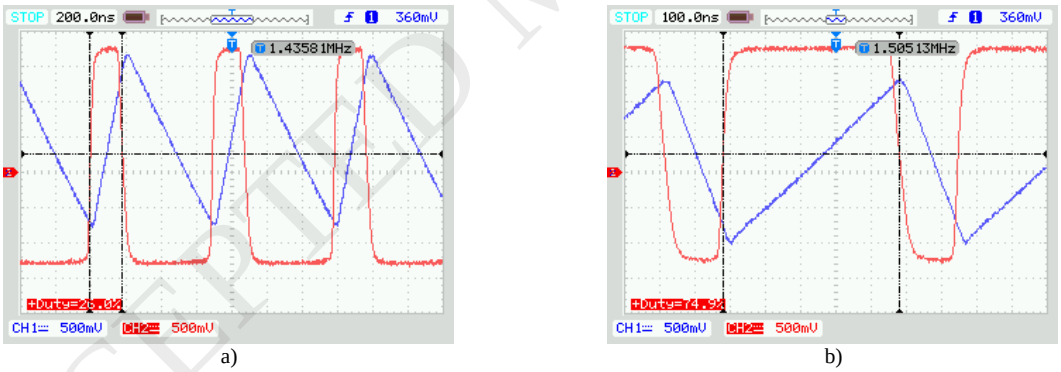

a) b)

Figure 29. Measured output transient responses (V_{SETA} = -1.35 V, V_{SETB} = 0.5 V): a) D = 26 % (V_{DUTY} = -0.9 V), b) D = 75 % (V_{DUTY} = +0.9 V).

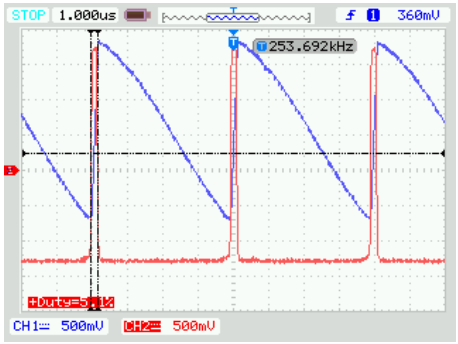

Figure 30. The example of minimal available D = 5.1 % for V_{DUTY} = -1.5 V.

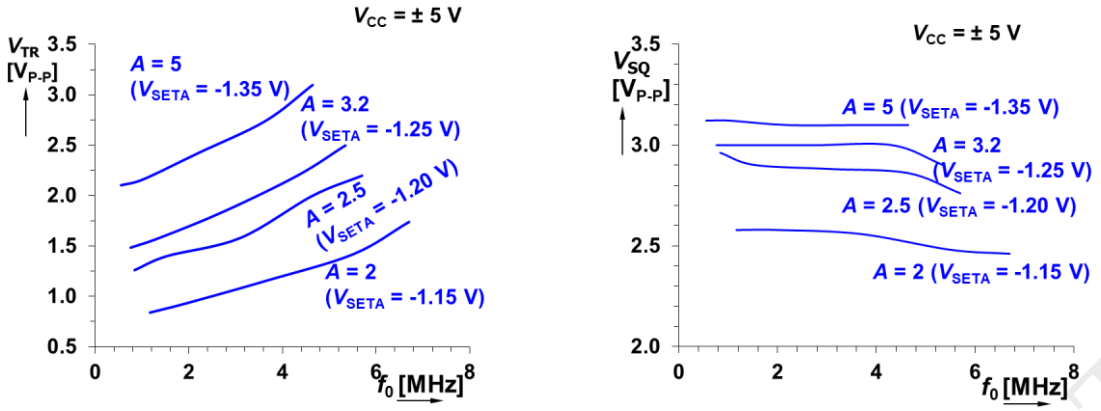

a) b)

Figure 31. Dependences of measured output levels on f_0 for various values V_{SETA}: a) triangular waveform output, b) square wave output.

6. Concluding remarks

Solution employing ECCII and VCA with adjustable duty cycle and repeating frequency was investigated in detail by simulations and laboratory experiments. Some of the results are summarized in **Tab. 2**. Detailed experimental results given for different operational conditions of comparator (VCA - different V_{SETA}) are summarized in **Tab. 3**. It can be seen that variation and inaccuracy of A (V_{SETA}) has significant effect on f_0 and output levels due to setting of threshold of the comparator. Nonlinearity when processing large signals and at high frequencies causes important differences in comparison to simulations and theoretical expectations (datasheet is showing only small-signal results).

Table 2. Comparison of the most important ideal, simulated and best fitting measured results.

	ideal	simulated	measured*
f_0 range [MHz] (V_{SETB} = 0.1→1.5 V)	0.64→9.67	0.63→7.05	0.85→6.00
D range [%] (V_{DUTY} = -0.9→+0.9 V)	5→95	8→93	26→75**
V_{SQ} [V_{P-P}]	N/A	2	3.0→2.8
V_{TR} [V_{P-P}]	N/A	1.6→1.9	1.3→2.2

* measured values for the best fitting setting (V_{SETA} = -1.20 V) with simulation results (V_{SETA} = -1.35 V)
** range 5→95 % is available for V_{DUTY} = -1.5→+1.5 V due to VCA non-idealities and nonlinearities

Table 3. Obtained laboratory results for different setting of V_{SETA} (different operational conditions) when changing gain B of integrator

V_{SETA} [V]	-1.15	-1.20	-1.25	-1.35
A [-]	2	2.5	3.2	5
V_{SETB} [V]	0.1→1.5			
B [-]	0.1→1.5			
f_0 [MHz]	1.16→6.70	0.85→6.00	0.76→5.35	0.55→4.65
f_{0max} : f_{0min}	5.8:1	7.1:1	7.0:1	8.5:1
V_{SQ} [V_{P-P}]	2.6→2.5	3.0→2.8	3→2.9	3.1
V_{TR} [V_{P-P}]	0.8→1.7	1.3→2.2	1.5→2.5	2.1→3.1

Statistical results of A dispersion show substantial influence on f_0 and D accuracy. The way how to move the frequency range to higher value is to reduce the gain A (as shown in **Tab. 3**, **Fig. 26**) at the expense of its worse accuracy and possible dispersion with fabrication tolerances or aging of components. Lower A allows to obtain quite high value of f_0 for relatively very low gain B (V_{SETB}) in the integrator (in values below 1). Low value of A also means advantageous frequency response of the VCA (because magnitude of A falls with –20 dB/dec). On the other hand, we can see that readjustability ratio of f_0 decreases with lower gain A, i.e. ratio f_{0max} : f_{0min} decreases for decreasing A.

New solution of the generator based on ECCII and VCA presented in **Fig. 2** has benefits and improved features in comparison to previous works (**Tab. 1**) as follows: a) minimal number of active and passive elements; b) voltage control of f_0 without impact on D; c) simple duty control by DC voltage V_{DUTY} and substantially lower

complexity of resulting circuits (additional circuit for $V \rightarrow I$ conversion to control D is not necessary as in works [13], [19]-[23] for example); d) presented circuit also does not suffer from practical limitation of dynamical features of integrator construction as indicated in [24] for example.

Despite inaccuracy between simulation and experimental results, both analyses confirmed expected impact of VCA gain (A) on the generator performance.

Acknowledgements

Research described in this paper was financed by Czech Ministry of Education in frame of National Sustainability Program under grant LO1401. For research, infrastructure of the SIX Center was used.

References

[1] D. Biolek, R. Senani, V. Biolkova, Z. Kolka, "Active elements for analog signal processing: Classification, Review and New Proposals Title of the paper," *Radioengineering*, vol. 17, no. 4, pp. 15-32, 2008.

[2] J. M. Jacob, "Analog Integrated Circuits Applications", New Jersey: Pretice-Hall, 2000.

[3] K. Kim, H-W. Cha, W-S. Chung, "OTA-R Schmitt trigger with independently controllable threshold and output voltage levels," *Electronics Letters*, vol. 33, no. 13, pp. 1103-1105, 1997.

[4] J. Misurec and J. Koton, "Schmitt Trigger with Controllable Hysteresis Using Current Conveyors," *International Journal of Advances in Telecommunications Electrotechnics, Signals and Systems*, vol. 1, no. 1, pp. 1-5, 2012.

[5] D. Biolek and V. Biolkova, "Current-mode CDTA-based comparators," in Proc. of the 13th Int. Conf. on Electronic Devices and Systems EDS-IMAPS, Brno, Czech Republic, 2006, pp. 6-10.

[6] A. De Marcellis, C. Di Carlo, V. Stornelli, "A CCII-based wide frequency range square waveform generator," *International Journal of Circuit Theory and Applications*, vol. 41, no. 1, pp. 1-13, 2013.

[7] H-Ch. Chien, "Voltage-controlled dual slope operation square/triangular wave generator and its application as a dual mode operation pulse width modulator employing differential voltage current conveyors," *Microelectronics Journal*, vol. 43, no. 12, pp. 962-974, 2012.

[8] B. Almashary and H. Alhokail, "Current-mode triangular wave generator using CCIIs," *Microelectronics Journal*, vol. 31, no. 4, pp. 239-243, 2000.

[9] D. Pal, A. Srinivasulu, B. B. Pal, A. Demosthenous, B. D. Das, "Current Conveyor-Based Square/Triangular Waveform Generators With Improved Linearity," *IEEE Transaction on Instrumentation and Measurement*, vol. 58, no. 7, pp. 2174-2180, 2009.

[10] AKM. S. Haque, M. M. Hossain, W. A. Davis, H. T. Russell, R. L. Carter, "Design of sinusoidal, triangular, and square wave generator using current feedback amplifier (CFOA)," in Proc. of IEEE Region 5 Conference, Kansas City, United States, 2008, pp. 1-5.

[11] Y. K. Lo and H. C. Chien, "Switch-controllable OTRA-based square/triangular waveform generator," *IEEE Transaction on Circuits Systems and Signal Processing II*, vol. 54, no. 12, pp. 1110-1114, 2007.

[12] S. Minaei and E. Yuce, "A simple Schmitt trigger circuit with grounded passive elements and its application to square/triangular wave generator," *Circuits, Systems, and Signal Processing*, vol. 31, no. 3, pp. 877-888, 2012.

[13] W. S. Chung, H. Kim, H-W. Cha, H-J. Kim, "Triangular/square-wave generator with independently controllable frequency and amplitude," *IEEE Transactions on Instrumentation and Measurement*, vol. 54, no. 1, pp. 105-109, 2005.

[14] M. Siripruchyanun and P. Wardkein, "A full independently adjustable, integrable simple current controlled oscillator and derivative PWM signal generator," *IEICE Trans. Fundam. Electron. Commun. Comput. Sci.*, vol. E86-A, no. 12, pp. 3119-3126, 2003.

[15] J. Kumbun and M. Siripruchyanun, "MO-CTTA-based electronically controlled current-mode square/triangular wave generator," in Proc. of the 1st International Conf. on Technical Education (ICTE2009), Bangkok, Thailand, 2010, pp. 158-162.

[16] P. Silapan and M. Siripruchyanun, "Fully and electronically controllable current-mode Schmitt triggers employing only single MO-CCCDTA and their applications," *Analog Integrated Circuits and Signal Processing*, vol. 68, no. 11, pp. 111-128, 2011.

[17] T. Srisakul, P. Silapan, M. Siripruchyanun, "An electronically controlled current-mode triangular/square wave generator employing MO-CCCCTAs," in Proc. of the 8th Int. Conf. on Electrical Engineering/ Electronics, Computer, Telecommunications, and Information Technology, Khon Kaen, Thailand, 2011, pp. 82-85.

[18] M. Janecek, D. Kubanek, K. Vrba, "Voltage-Controlled Square/Triangular Wave Generator with Current Conveyors and Switching Diodes," *International Journal of Advances in Telecommunications Electrotechnics, Signals and Systems*, vol. 1, no. 2-3, pp. 1-4, 2012.

[19] R. Sotner, J. Jerabek, N. Herencsar, "Voltage Differencing Buffered/ Inverted Amplifiers and Their Applications for Signal Generation," *Radioengineering*, vol. 22, no. 2, pp. 490-504, 2013.

[20] R. Sotner, J. Jerabek, N. Herencsar, T. Dostal, K. Vrba, Design of Z-copy controlled-gain voltage differencing current conveyor based adjustable functional generator, Microelectronics Journal, vol. 46, no. 2, pp. 143-152, 2015.

[21] J. Jerabek, R. Sotner, T. Dostal, K. Vrba, Simple Resistor-less Generator Utilizing Z-copy Controlled Gain Voltage Differencing Current Conveyor for PWM Generation, Elektronika Ir Elektrotechnika, vol. 21, no. 5, pp. 28-34, 2015.

[22] R. Sotner, J. Petrzela, J. Jerabek, O. Domansky, L. Langhammer, Special Electronically Reconfigurable Lossy/Lossless Integrator in Application of Functional Generator, in proc. of 27th International Conference Radioelektronika 2017, pp. 1-5, 2017.

[23] R. Sotner, J. Jerabek, N. Herencsar, R. Prokop, K. Vrba, J. Petrzela, T. Dostal, "Simply Adjustable Triangular and Square Wave Generator Employing Controlled Gain Current and Differential Voltage Amplifier," in Proc. Of the 23th Int. Conf. Radioelektronika 2013, Pardubice, Czech Republic, 2013, pp. 109-114.

[24] R. Sotner, J. Jerabek, N. Herencsar, A. Lahiri, J. Petrzela, K. Vrba, "Practical Aspects of Operation of Simple Triangular and Square Wave Generator Employing Diamond Transistor and Controllable Amplifiers," in Proc. Of the 36th Int. Conf. on Telecommunications and Signal Processing (TSP2013), Rome, Italy, 2013, pp. 431-435.

[25] Texas Instruments. VCA810 High gain adjust range, wideband, variable gain amplifier (online), Available from: http://www.ti.com/lit/ds/symlink/vca810.pdf

[26] J. Jerabek, R. Sotner, K. Vrba, "Fully-differential current amplifier and its application to universal and adjustable filter," in Proceedings of the International Conference on Applied Electronics APPEL2010, Pilsen, 2010, pp. 141-144.

[27] R. Sotner, J. Jerabek, N. Herencsar, Z. Hrubos, T. Dostal, K. Vrba, "Study of Adjustable Gains for Control of Oscillation Frequency and Oscillation Condition in 3R-2C Oscillator," *Radioengineering*, vol. 21, no. 1, pp. 392-402, 2012.

[28] R. Sotner, Z. Hrubos, B. Sevcik, J. Slezak, J. Petrzela, T. Dostal, "An example of easy synthesis of active filter and oscillator using signal flow graph modification and controllable current conveyors," *Journal of Electrical Engineering*, vol. 62, no. 5, pp. 258-266, 2011.

[29] R. Sotner, A. Lahiri, A. Kartci, N. Herencar, J. Jerabek, K. Vrba, "Design of Novel Precise Quadrature Oscillators Employing ECCIIs with Electronic Control," *Advances in Electrical and Computer Engineering*, vol. 13, no. 2, pp. 65-72, 2013.

[30] Intersil (Elantec). EL2082 CN Current-mode multiplier (online), Available from: http://www.intersil.com/data/fn/fn7152.pdf

[31] W. Surakampontorn and W. Thitimajshima, "Integrable electronically tunable current conveyors," *IEE Proceedings-G*, vol. 135, no. 2, pp. 71-77, 1988.

[32] A. Fabre and N. Mimeche, "Class A/AB Second-generation Current Conveyor with Controlled Current Gain," *Electronics Letters*, vol. 30, no. 16, pp. 1267-1268, 1994.

[33] S. Minaei, O. K. Sayin, H. Kuntman, "A new CMOS electronically tunable current conveyor and its application to current-mode filters," *IEEE Trans. on Circuits and Systems - I*, vol. 53, no. 7, pp. 1448-1457, 2006.